

## Osteopontin is a downstream effector of the PI3-kinase pathway in melanomas that is inversely correlated with functional PTEN

Leisl Packer\*, Sandra Pavey, Andrew Parker<sup>1</sup>,  
Mitchell Stark, Peter Johansson<sup>2</sup>, Belinda Clarke<sup>3</sup>,  
Pamela Pollock<sup>4</sup>, Markus Ringner<sup>2</sup> and  
Nicholas Hayward

Human Genetics Laboratory, Queensland Institute of Medical Research, Herston 4006, QLD, Australia, <sup>1</sup>Department of Cellular Pathology, John Radcliffe Hospital, Oxford OX3 9DU, UK, <sup>2</sup>Department of Theoretical Physics, Lund University, Lund SE-223 62, Sweden, <sup>3</sup>Queensland Health Pathology Services, Prince Charles Hospital, Brisbane 4032, Australia and <sup>4</sup>Melanoma Genetics Research Unit, Translational Genomics Research Institute, Phoenix 85004, USA

\*To whom correspondence should be addressed. Tel: +61 7 3362 0308;  
Fax: +61 7 3845 3508;  
Email: Leisl.Packer@qimr.edu.au

**The tumor suppressor PTEN antagonizes phosphatidylinositol 3-kinase (PI3K), which contributes to tumorigenesis in many cancer types. While *PTEN* mutations occur in some melanomas, their precise mechanistic consequences have yet to be elucidated. We sought to identify novel downstream effectors of PI3K using a combination of genomic and functional tests. Microarray analysis of 53 melanoma cell lines identified 610 genes differentially expressed ( $P < 0.05$ ) between wild-type lines and those with *PTEN* aberrations. Many of these genes are known to be involved in the PI3K pathway and other signaling pathways influenced by PTEN. Validation of differential gene expression by qRT-PCR was performed in the original 53 cell lines and an independent set of 18 melanoma lines with known *PTEN* status. Osteopontin (OPN), a secreted glycoprophosphoprotein that contributes to tumor progression, was more abundant at both the mRNA and protein level in *PTEN* mutants. The inverse correlation between OPN and *PTEN* expression was validated ( $P < 0.02$ ) by immunohistochemistry using melanoma tissue microarrays. Finally, treatment of cell lines with the PI3K inhibitor LY294002 caused a reduction in expression of OPN. These data indicate that OPN acts downstream of PI3K in melanoma and provides insight into how *PTEN* loss contributes to melanoma development.**

### Introduction

The *PTEN* tumor suppressor is a dual-specificity phosphatase that is mutated or lost in a number of sporadic and familial cancers (1). The growth suppressive effects of *PTEN* are thought to result from its lipid phosphatase function, which inhibits activation of the phosphatidylinositol 3-kinase (PI3K)

pathway, responsible for promoting cell growth, survival and tumorigenesis when overstimulated (2,3). *PTEN* also acts as a protein phosphatase, modulating targets such as focal adhesion kinase (FAK) and cyclin D1 (4,5). This function of *PTEN* has been shown to oppose cell migration and promote cell growth arrest (6,7). Therefore, cells lacking functional *PTEN* have increased proliferation, altered migration and reduced apoptosis. Additionally, Waite and Eng (8) allude to the possibility that *PTEN* is involved in other cell functions not yet identified. To further understand the role of *PTEN* in normal and malignant cells, additional targets that are inappropriately activated when *PTEN* is mutated need to be identified. Because the main tumor-promoting effect resulting from *PTEN* inactivation is initiated through PI3K upregulation, we sought to identify downstream components of this pathway that are upregulated when *PTEN* is lost. Such gene products have the potential to act as effectors of cell growth and proliferation when *PTEN* is inactive and may therefore act as targets for therapeutic intervention in the treatment of cancers with *PTEN* mutations. Similar to the MAPK signal transduction pathway, the PI3K pathway is constitutively active in melanomas and is therefore an important target of anticancer treatments (9). Active PI3K regulates a number of neoplasia-associated processes in melanoma, including proliferation, apoptosis, cell migration and vascular mimicry (10–12).

Using microarray gene expression profiling followed by functional analysis, we identified osteopontin (OPN) as a downstream effector of PI3K in melanoma cell lines with inactive *PTEN*. OPN is a secreted glycoprophosphoprotein involved in a number of cell functions including cell adhesion and migration, anti-apoptosis, inflammation, angiogenesis, bone calcification and anchorage-independent growth of tumor cells (13–17). Many studies have found OPN to be overexpressed in cancer compared with corresponding normal tissue, with increased expression found to correlate with tumor burden and invasive ability in a variety of experimental models (18–25).

The importance of OPN in tumor growth and metastasis has been demonstrated in studies showing that increased levels stimulated invasion, cell proliferation and colony growth *in vitro* (26,27) and tumor growth, angiogenesis and metastasis *in vivo* (28–30); whereas, inhibition of OPN resulted in a reduction in these cancer-promoting processes (31–35). A number of studies support the involvement of OPN in melanoma development (35–38). Of particular interest are three independent microarray expression studies that found an increase in *OPN* expression in melanoma cells compared with normal and benign melanocytes, and in metastatic melanomas compared with primary lesions (39–41).

The present study provides evidence of a link between *PTEN* loss and increased *OPN* expression at both the mRNA and protein level that involves PI3K activation of *OPN* and which may help explain how *PTEN* loss promotes increased cell migration, growth and invasion.

**Abbreviations:** DMSO, dimethyl sulfoxide; GOs, gene ontologies; OPN, osteopontin; PI3K, phosphatidylinositol 3-kinase; qRT-PCR, quantitative reverse transcriptase-polymerase chain reaction; TMA, tissue microarray; WT, wild-type.

## Materials and methods

### Cell culture and RNA extraction

The 53 melanoma cell lines used in this study were derived from primary cutaneous melanomas or their metastases and cultured as described previously (42). Qiagen RNeasy Midi-kits were used to extract total RNA from cells in log phase growth according to the manufacturer's instructions.

### Genotyping of cell lines

A number of mutations have previously been documented in exons 1–8 of the *PTEN* gene, with a large number located within exon 5, which encodes the well-conserved phosphatase core motif (43). Here, exons 1–9 of *PTEN* were amplified separately using primers described in Supplementary Table 1 and sequenced according to the methods described in Supplementary Methods 1.

### Microarray methods

Microarray hybridization and washing was performed as described previously (42) using Human 19K Arrays (v2.0) obtained from the Microarray Centre, University Health Network, Ontario, Canada. See Supplementary Methods 2 for further information.

### Gene ontology analysis

The Gene Ontologies (GOs) of genes in the *PTEN* differential expression gene list ( $n = 610$ ) were analyzed using DAVID v1.0 (44) and EASE v2.0 (45). The biological functions were requested from DAVID at a specificity level of 5 (high specificity, low coverage).

### Quantitative RT-PCR

To confirm the validity of the microarray expression data, the mRNA levels of 20 unique transcripts selected from the  $P < 0.05$  microarray gene list ( $n = 610$ ) were assessed by quantitative reverse transcriptase–polymerase chain reaction (qRT-PCR) (see Supplementary Table 6 for primer sequences and Supplementary Methods 3 for PCR conditions). *GAPDH* was chosen as the normalization control transcript, as it showed minimal variation in the microarray hybridizations (within 0.7–1.4-fold of the reference value in all samples). The reference melanoma cell line MM329 was used to establish the amplification efficiencies of each gene (46). cDNA was made using Superscript III reverse transcriptase (Invitrogen, CA, USA). Subsequent PCR reactions were carried out on a Corbett RotorGene 3000 (Corbett Research, Australia) using SYBR Green RT-PCR Master Mix (Applied Biosystems, Foster City, CA) or QuantiTect SYBR Green PCR mix (Qiagen, Germany). Reference and test cell lines were amplified in parallel reactions using specific primers. Specificity of PCR products obtained was characterized by melting curve analysis. Gel electrophoresis and DNA sequencing and/or restriction enzyme digestion were carried out on PCR products for each primer set to confirm identity.

### Western blotting

*PTEN* genotype status was confirmed by western blotting of melanoma cell line protein extracts using a 1:1000 dilution of the *PTEN* antibody 6H2.1 (Cascade Biosciences, MA, USA). The specificity of this antibody has been confirmed previously (47–49). Activation of the PI3K pathway was also determined by staining with a phospho-Akt (Ser473) antibody (Cell Signaling Technology, MA, USA) diluted 1:1000. Detection of OPN secreted from the melanoma cell lines was performed as follows:  $1.5 \times 10^6$  cells were seeded into 25 cm<sup>2</sup> flasks and allowed to adhere in RPMI1640 containing 10% FCS over 3–5 h. Once cells had adhered to the flask, 5 ml RPMI1640 medium (without serum) were added to the cells and aspirated after 16 h for analysis of OPN. Crude medium (30  $\mu$ l) together with 3  $\mu$ l sample loading buffer were electrophoresed through a 10% acrylamide gel. Western blots were probed overnight at 4°C with anti-OPN antibody (Abcam, UK) diluted 1:1000 in 2.5% bovine serum albumin (BSA). Equal loading of samples was confirmed using Coomassie blue staining of the gel post-transfer (data not shown). See Supplementary Methods 4 for further details.

### Inhibition of PI3K

Two cell lines (D20 and HT144) carrying mutant *PTEN* were treated with 50  $\mu$ M LY294002 in dimethyl sulfoxide (DMSO) (Cell Signaling Technology) in triplicate experiments. A vehicle control (DMSO) was performed along with each LY294002-treated sample. Cells were grown in 10 cm<sup>2</sup> plates and collected for RNA and protein at 7 h post-treatment. Cells were lysed in 350  $\mu$ l RLT buffer, and RNA and protein were extracted as described in Supplementary Methods 4. To confirm inhibition of PI3K activity, protein was run on a 10% acrylamide gel and probed with the phospho-Akt antibody.

### Melanoma tissue microarray (TMA)

Paraffin-embedded formalin-fixed tissue blocks were obtained from the Prince Charles Hospital after approval by the Hospital's Human Research Ethics

Committee. The most representative malignant or benign area was selected by a pathologist and marked on the H&E-stained slide. A Manual Tissue Arrayer-1 (MTA-1) from Beecher Instruments (USA) was used to construct the arrays, which consisted of 1.5 mm diameter cores. The TMAs were constructed using punch biopsies from 105 primary melanomas, 96 nevi and 21 metastatic melanomas. However, owing to loss of biopsy cores during array processing or the absence of melanocytic cells, scoring for both *PTEN* and *OPN* staining using 4  $\mu$ m sections cut from the TMA was obtained for only 67 primary melanomas, 29 nevi and 19 metastatic melanomas. The TMA slides were processed and stained as described in the Supplementary Methods 5. Antibodies used were monoclonal *PTEN* (clone 6H2.1, Cascade Biosciences) diluted 1:200 and monoclonal *OPN* (MPIIB10<sub>1</sub>) diluted 1:100. The *OPN* monoclonal antibody developed by Michael Solorsh and Anders Franzen was obtained from the Developmental Studies Hybridoma Bank developed under the auspices of the NICHD and maintained by The University of Iowa, Department of Biological Sciences, Iowa City. This antibody was shown by western blotting (data not shown) to recognize full-length *OPN*, as well as a number of faster migrating species. The multiple bands observed probably represent various levels of post-translational modifications of the full-length protein, including phosphorylation and glycosylation. It is not known whether this antibody detects all phosphorylated and glycosylated forms of *OPN*.

### Immunohistochemical scoring

The stained TMAs were scored separately for staining intensity (I) on a four-point scale (a score of 0 indicating no staining, 1 = weak staining, 2 = moderate staining and 3 = strong staining) and the proportion of positive cells (P) on a scale of 0.0–1.0, where 1.0 indicates 100% of cells stained. The histologic or H-score (50) was then calculated. This is the product of the intensity and proportion of melanocytic cells stained ( $H = I \times P$ ). The H-score ranged from 0.0 to 3.0, with 0 indicating negative staining in all cells and 3.0 indicating strong staining in 100% of cells. The non-parametric Spearman's test was used to determine the correlation between expression of *PTEN* and *OPN*.

## Results

### *PTEN* mutation status and protein expression

The mutation status of *PTEN* was determined for each cell line (see Supplementary Tables 2a and 2b). For the initial set of 53 melanoma cell lines, mutations or deletions in the following cell lines have been described previously (51): MM622, BL, MM386, C-32, HT144, A2058 and MM200. Two additional cell lines, D14 and D20, were also found to have homozygous deletions.

The *PTEN* genotype status was confirmed at the protein level using western blotting. Cell lines identified as having mutated/deleted *PTEN* failed to express *PTEN* protein, whereas *PTEN* was detected in all cell lines containing wild-type (WT) *PTEN*. A representative blot is shown in Figure 1A. We found that both A2058 and MM200 lacked *PTEN* protein, suggesting that their missense mutations (L112Q, L186M in A2058 and F56I in MM200) render *PTEN* inactive. The original set of 53 melanoma cell lines was thus grouped into 9 mutant *PTEN* and 44 WT *PTEN*.

Of the 18 melanoma cell lines in the validation set, 10 contained WT *PTEN*. Homozygous deletions of *PTEN* were found in six cell lines: A06, A13, D36, MM488, MM604 and D32, all of which failed to express *PTEN* protein. The splice mutation in AF-6 and the missense variant (T167A) in SKMEL-28 were reported previously (51). *PTEN* protein was absent for AF-6, whereas SKMEL-28 expressed *PTEN* at normal levels and showed no AKT activation (Supplementary Figure 2) and was therefore placed in the WT group as it appeared to have functional *PTEN*. Thus, in the second set of melanoma cell lines, the mutant group contained 7 cell lines, with the remaining 11 cell lines containing WT *PTEN*. The presence of *PTEN* protein in all WT cell lines indicates that the *PTEN* protein is not lost by other mechanisms, such as promoter methylation.

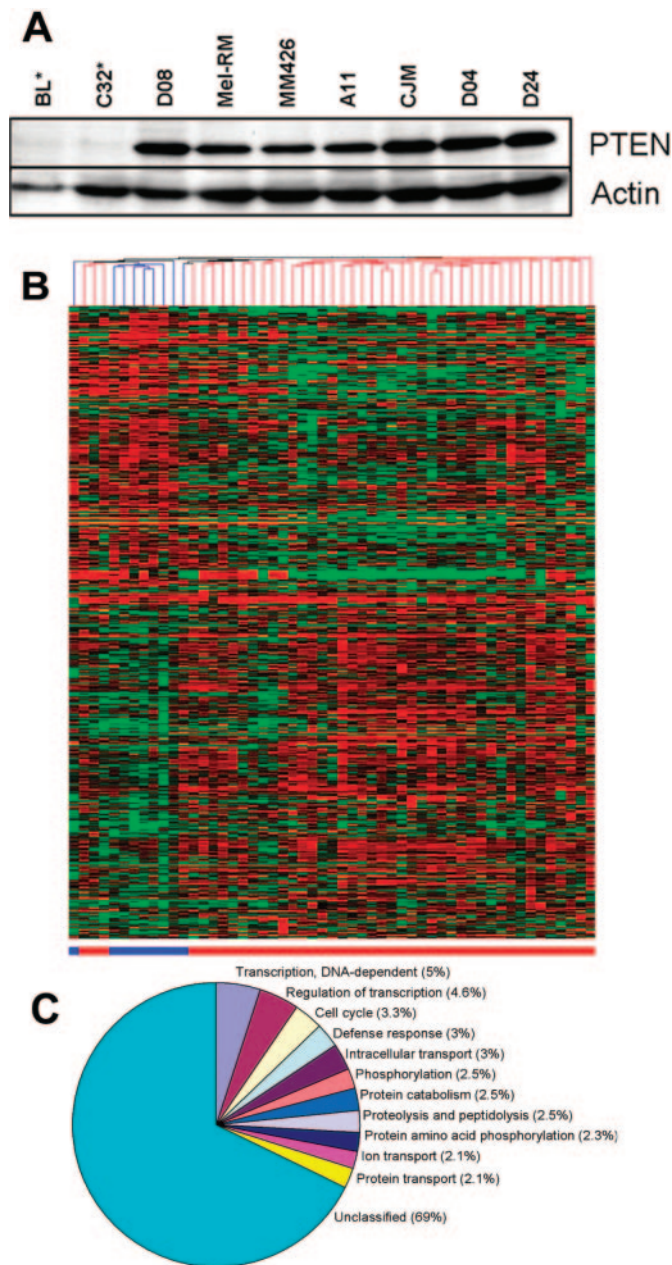


**Fig. 1.** (A) Expression of *PTEN* in melanoma cell lines by western blot analysis. Asterisk indicates cell lines containing mutated/deleted *PTEN*. (B) Hierarchical clustering of 53 melanoma cell lines and genes, using the gene list containing 610 genes identified as being differentially expressed between the *PTEN* mutant group (blue) and *PTEN* WT group (red) by ANOVA at a  $P$ -value of 0.05. Pearson's correlation was used to cluster the samples (vertical branch structure) and genes (presented horizontally) based on centralized data. (C) Division of *PTEN* differential gene list ( $n = 610$ ) based on GO using biological process classification as determined by DAVID.

Detection of AKT activation in all cell lines was achieved by staining western blots for phospho-Akt, the immediate downstream target of PI3K (Supplementary Figure 2). The majority of cell lines expressing *PTEN* had little or no phospho-Akt present and those cell lines lacking *PTEN* generally showed high levels of phospho-Akt, which is consistent with what is known about the activation of the PI3K pathway with *PTEN* loss. However, the inverse correlation was not absolute, with a number of cell lines (D08, D04, MM608 and MM409)

expressing both *PTEN* and phospho-Akt. Interestingly, these cell lines carry activating mutations in *NRAS* or *BRAF* (data not shown), which may explain the activation of AKT independent of *PTEN* loss. Western blot analysis also showed a single cell line (C-32) without *PTEN* or phospho-Akt. These results are supported by Curtin *et al.* (52), who found that phospho-Akt was not always present when *PTEN* is lost, though the majority of samples showed a negative correlation between *PTEN* and phospho-Akt.

#### Supervised gene selection

To identify genes differentially expressed between cell lines containing WT or mutant *PTEN* the non-parametric Wilcoxon–Mann–Whitney  $U$ -test was performed on the microarray data. Using a filtered list of 12 490 genes, 610 genes at  $P < 0.05$  and 96 genes at  $P < 0.01$  were found to be differentially expressed between the two groups (Supplementary Table 3a and b). We hypothesized that a number of genes on the differential expression gene list might represent biological effectors of *PTEN*, even though no overabundance of differentially expressed genes was found compared with the number expected purely by chance. Examination of the gene list showed many genes with strong expression differences between the two genotypic groups, as well as functions that could contribute to tumorigenesis resulting from loss of *PTEN*. To test this hypothesis, differentially expressed genes were investigated in an independent set of cell lines.

Hierarchical clustering using the 610 discriminatory genes from the  $P < 0.05$  gene list was performed in both the sample and transcript dimensions (Figure 1B). Clustering of cell lines based on their expression of these genes shows good separation of the cell lines with mutant and WT *PTEN*, thereby showing that many of these genes are expressed in concordance with *PTEN* status.

#### Ontology analysis

The breakdown of the *PTEN* ( $n = 610$ ) gene list into GOs using DAVID is shown in Figure 1C. GOs of relevance to the *PTEN* pathway include DNA-dependent transcription, regulation of transcription, cell cycle, intracellular transport, phosphorylation and protein transport (full GO categorization of the gene list is detailed in Supplementary Table 4a and b). EASE analysis was then performed using the gene symbol categorization of clones to determine which GOs were overrepresented in the differentially expressed gene list ( $n = 610$ ,  $P < 0.05$ ) compared with the filtered gene list ( $n = 12,940$ ). Two GOs, response to stress (GO:0006950) and negative regulation of transcription (GO:0016487), were significantly ( $P < 0.05$ ) overrepresented in association with *PTEN* aberrations (Supplementary Table 5).

#### Quantitative RT-PCR

The expression of 20 genes selected from the microarray data was validated using qRT-PCR. Genes were selected on the basis of their differential expression between the *PTEN* WT and mutant groups. The correlation between the qRT-PCR and the microarray expression levels was determined for each of the genes using the Spearman's test (see Table I and Supplementary Tables 7a–t for raw data). Of the 20 genes assessed by qRT-PCR in the original set of 53 cell lines, the expression distribution between the two groups was confirmed for 18 genes (only *GSK3B* and *PRSS11* did not reach statistical significance). A subset of 9 genes was subsequently verified in the independent set of 18 melanoma cell lines, including

**Table I.** Comparison of qRT-PCR and microarray expression data for 20 genes selected for validation

Gene	No. of cell lines	Microarray		qRT-PCR		Ratio MUT/WT		Spearman correlation*		No. of cell lines	Second set MM lines			Expression difference confirmed
		Mean WT	Mean MUT	Mean WT	Mean MUT	Microarray	qRT-PCR	R	P		WT	MUT	MUT/WT	
<i>AF1Q</i>	18	2.657	4.487	7.445	12.270	1.688	1.648	0.608	0.007	12	9.840	2.522	0.256	N
<i>BCL3</i>	48	2.659	4.812	5.722	11.576	1.810	2.023	0.683	<0.001	16	6.323	12.985	2.054	Y
<i>COL1A2</i>	26	2.580	12.820	1.306	22.186	4.969	16.984	0.755	<0.001	18	79.506	21.702	0.273	N
<i>CYFIP2</i>	18	1.542	0.250	2.277	0.313	0.162	0.137	0.871	<0.001	17	0.953	1.531	1.607	N
<i>GAS7</i>	46	1.224	2.289	1.258	1.933	1.870	1.537	0.822	<0.001	16	0.020	0.014	0.700	N
<i>GSK3B</i>	43	1.333	1.765	1.333	0.996	1.324	0.748	-0.017	NS	17	1.355	1.82	1.342	N
<i>HEY1</i>	48	2.274	3.249	2.274	3.521	1.429	1.548	0.308	0.033	15	2.488	5.202	2.091	Y
<i>ITGB3</i>	49	0.957	1.441	0.662	1.162	1.506	1.755	0.604	<0.001	14	0.810	2.701	3.334	Y
<i>LAF4</i>	50	1.452	0.976	1.397	0.461	0.672	0.330	0.309	0.029	15	0.781	0.807	1.033	N
<i>NFKB1</i>	24	0.853	1.292	0.492	0.780	1.514	1.584	0.537	0.007	17	0.855	1.099	1.286	Y
<i>NRBF1</i>	24	1.209	0.677	1.507	0.828	0.560	0.549	0.512	0.011	18	1.138	1.721	1.512	N
<i>OPN</i>	47	8.359	16.579	2.802	4.443	1.983	1.585	0.894	<0.001	15	2.326	16.320	7.016	Y
<i>PAK4</i>	23	0.994	2.141	1.022	1.958	2.153	1.917	0.589	0.002	17	1.622	1.062	0.655	N
<i>PRSS11</i>	28	0.590	0.922	1.827	4.832	1.562	2.645	0.138	NS	14	1.976	1.398	0.708	N
<i>RELB</i>	44	0.964	1.822	4.025	3.531	1.890	0.877	0.450	0.002	17	4.569	6.785	1.485	N
<i>RPS6KA2</i>	52	1.114	0.209	4.038	0.330	0.188	0.082	0.638	<0.001	18	1.730	0.387	0.223	Y
<i>STAT3</i>	47	2.186	2.612	0.944	1.161	1.195	1.230	0.436	0.002	15	0.782	1.873	2.395	Y
<i>STIM2</i>	49	0.734	1.241	0.448	0.640	1.690	1.430	0.570	<0.001	14	0.346	0.916	2.650	Y
<i>TRAP1</i>	21	0.874	0.576	1.039	0.396	0.659	0.381	0.546	0.010	18	0.560	0.548	0.977	Y
<i>ZFYVE26</i>	30	0.756	0.471	1.026	0.492	0.624	0.480	0.650	<0.001	18	3.980	10.479	2.633	N

Results are expressed as the ratio of gene of interest/GAPDH. The ratio of MUT/WT is the mean expression ratio in PTEN mutant (MUT) samples/mean expression ratio in PTEN WT samples. qRT-PCR was performed on 7–9 PTEN mutant samples and between 9 and 43 randomly selected samples containing WT PTEN.

\*Spearman correlation used to compare associations between the MUT/WT ratios of the microarrays and qRT-PCR.

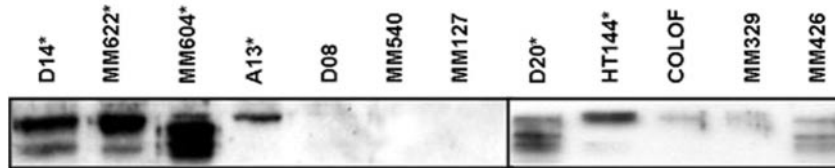


**Fig. 2.** Analysis of secreted OPN by western blotting of conditioned media. Asterisk indicates cell line with mutant *PTEN*.

*BCL3*, *HEY1*, *ITGB3*, *NFKB1*, *OPN*, *RPS6KA2*, *STAT3*, *STIM2* and *TRAP1*. Four of these genes (*BCL3*, *ITGB3*, *STAT3* and *NFKB1*) are known to function downstream of the PI3K pathway, and as expected with increased PI3K signaling, these genes showed higher expression in the PTEN mutant group.

From the list of nine genes confirmed in both sets of cell lines, *OPN* was selected for further functional analysis. Selection was based on the strong differential expression of *OPN* between the two groups and its potential role in melanoma progression (41). Using a representative panel of cell lines ( $n = 64$ ) from both the original 53 and validation set of 18, *OPN* mRNA was on average 3.4-fold more abundant in the mutant group compared with the WT group ( $P < 0.01$ ).

#### Detection of *OPN* secreted from melanoma cell lines

The amount of secreted OPN was determined by western blots of conditioned media (Figure 2). The level of secreted OPN was substantially greater in cell lines containing mutant PTEN, consistent with the mRNA expression data. The multiple bands are likely to be OPN isoforms with various degrees of phosphorylation and glycosylation, which have been observed previously, although it is possible that the antibody used does not detect all species (53,54).

#### *PI3K inhibition by LY294002*

The cell lines HT144 and D20 were chosen to undergo LY294002-treatment based upon the absence of PTEN and the presence of activated phospho-Akt in these cells (see Supplementary Figure 2). Treatment with LY294002 for 7 h was shown to abrogate the activity of PI3K, as shown in western blots stained with a phospho-Akt antibody (Figure 3A). To determine whether *OPN* is downstream of the PI3K pathway, qRT-PCR was used to measure transcript levels in treated cells compared with DMSO-treated cells (Figure 3B). Using a paired *t*-test, the reduction of *OPN* in D20 was significant at a *P*-value of 0.05, and a similar trend was seen in HT144. These results suggest that *OPN* is downstream of the PI3K pathway and that transcription of *OPN* is increased upon activation of AKT.

#### TMA staining

Protein staining of PTEN and OPN was assessed in a variety of benign nevi, primary melanomas and metastatic melanomas (Table II). PTEN was expressed ( $H > 0.7$ ) in 41% of nevi, 67% of primary melanomas and 37% of metastatic melanomas, whereas little or no PTEN ( $H < 0.7$ ) was observed in the remaining samples. There are two conflicting studies regarding PTEN expression in nevi, with one showing cytoplasmic

PTEN in almost all benign nevi (55) and the other with no PTEN staining in any benign nevi (56). The use of different antibodies is likely to result in different PTEN staining, though in considering these previous reports and the results presented in this study, it is difficult to draw conclusions on the role of PTEN in benign nevi. The incidence of PTEN loss in primary melanomas was similar to that observed in previous studies (55,57,58). Among the primary melanomas no correlation

was found between PTEN staining and Breslow thickness or Clarke Level, in keeping with our previous findings (58).

OPN staining was observed in the cytoplasm of the majority of melanoma cells, and interestingly, in many samples OPN also appeared to be concentrated in small defined spots immediately adjacent to the nucleus. This punctate staining pattern is likely to be OPN in the golgi apparatus and secretory vesicles, as previous studies have shown co-localization of OPN to these subcellular structures (59–61). Punctate staining of OPN was most variable between lesions and was therefore scored and included in the correlation tests. Cytoplasmic OPN was expressed at moderate to high levels ( $H > 0.7$ ) in 41, 91 and 68% of benign nevi, primary melanomas and metastatic melanomas, respectively. The increased expression of OPN in primary melanomas compared with benign nevi was also noted by Zhou *et al.* (41). We also found no significant difference between OPN expression in primary and metastatic melanomas ( $P > 0.05$ , *t*-test). Similar to PTEN, no correlation was found between OPN staining and Breslow thickness or Clarke Level. The lack of correlation between PTEN and OPN staining with these histopathological features is consistent with previous findings (58). Representative immunohistochemistry (IHC) photographs of melanomas taken from the TMA showing staining for PTEN and OPN are shown in Figure 4.

Correlations between PTEN and OPN expression (cytoplasmic and punctate) in the primary melanomas ( $n = 67$ ) were then assessed using the non-parametric Spearman's test (Table III). To achieve a single value for OPN staining that accounted for both the punctate and cytoplasmic OPN, a composite score was calculated by multiplying the punctate OPN score with the cytoplasmic OPN score. This was done for all three scoring variables: percentage of cells stained, intensity of staining and the H-score. Significant ( $P < 0.02$ ) inverse correlations were evident between PTEN and both the OPN composite score and OPN punctate staining when examining the percentage of cells stained and the H-score. No significant correlations were identified between the intensity of staining of PTEN and OPN. The increase in OPN together with the absence of PTEN was not associated with Breslow thickness or Clarke Level, suggesting that the correlation is not associated with melanoma progression.

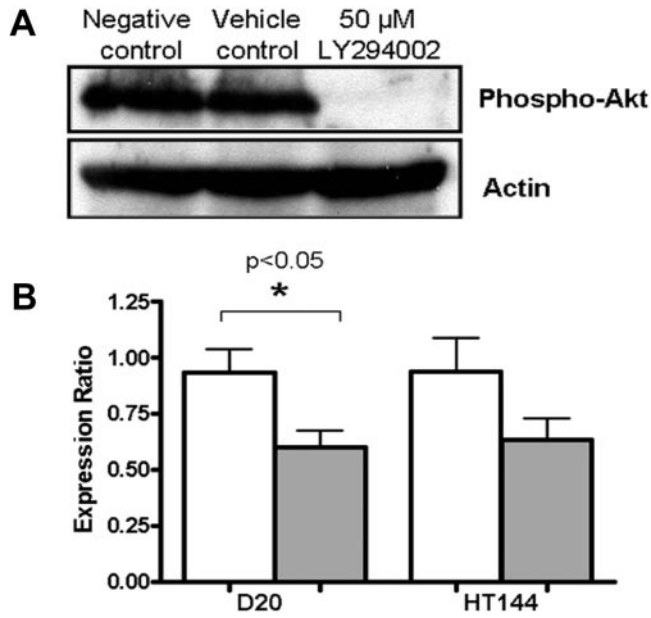


**Fig. 3.** (A) Western blots showing phospho-Akt status of the melanoma cell line D20 negative control, vehicle control (DMSO) and cells treated with 50  $\mu$ M LY294002 for 7 h. Actin was used as a loading control. (B) mRNA expression of *OPN* in the melanoma cell lines D20 and HT144 at 7 h post-treatment with 50  $\mu$ M LY294002. *OPN* expression in the vehicle control (DMSO) is shown by open bars and that in the LY294002-treated samples is shown by the shaded bars. Expression was normalized using GAPDH. The mean of three independent experiments is presented and error bars indicate standard error of the mean. Asterisk indicates level of *OPN* is significantly different between vehicle control and treated cells at a level of  $P < 0.05$ .

**Table II.** OPN and PTEN staining of benign nevi, primary melanomas and metastatic melanomas, as determined by each scoring method (percentage of cells stained, intensity of staining and a composite score of both, reported as the H-score)<sup>a</sup>

Category	PTEN staining			OPN punctate staining			OPN cytoplasmic staining		
	Benign (%)	Primary melanoma (%)	Metastatic melanoma (%)	Benign (%)	Primary melanoma (%)	Metastatic melanoma (%)	Benign (%)	Primary melanoma (%)	Metastatic melanoma (%)
Percent of cells stained (P)									
<25%	16 (55)	21 (31)	11 (58)	5 (17)	25 (37)	7 (37)	14 (48)	6 (9)	2 (11)
25–75%	1 (4)	5 (8)	–	19 (66)	24 (36)	4 (21)	–	–	1 (5)
>75%	12 (41)	41 (61)	8 (42)	5 (17)	18 (27)	8 (42)	15 (52)	61 (91)	14 (48)
Intensity of staining (I)									
Negative	14 (48)	14 (21)	12 (63)	–	4 (6)	–	14 (48)	6 (9)	2 (11)
Weak	4 (14)	24 (36)	1 (5)	6 (21)	9 (13)	3 (16)	13 (45)	37 (55)	17 (89)
Moderate	6 (21)	22 (33)	4 (21)	23 (79)	51 (76)	11 (58)	2 (7)	20 (30)	–
Strong	5 (17)	7 (10)	2 (11)	–	3 (4)	5 (26)	–	4 (6)	–
H-score ( $H = P \times I$ )									
0.0–0.7	17 (59)	22 (33)	12 (63)	12 (41)	28 (42)	8 (42)	17 (59)	6 (9)	4 (21)
0.8–1.5	3 (10)	22 (33)	1 (5)	14 (48)	22 (33)	4 (21)	10 (34)	37 (55)	13 (68)
1.6–3.0	9 (31)	23 (34)	6 (32)	3 (10)	17 (25)	7 (37)	2 (7)	24 (36)	–
TOTAL	29	67	19	29	67	19	29	67	19

<sup>a</sup>Each method of scoring was categorized and the number of samples with staining in each of the categories is shown.

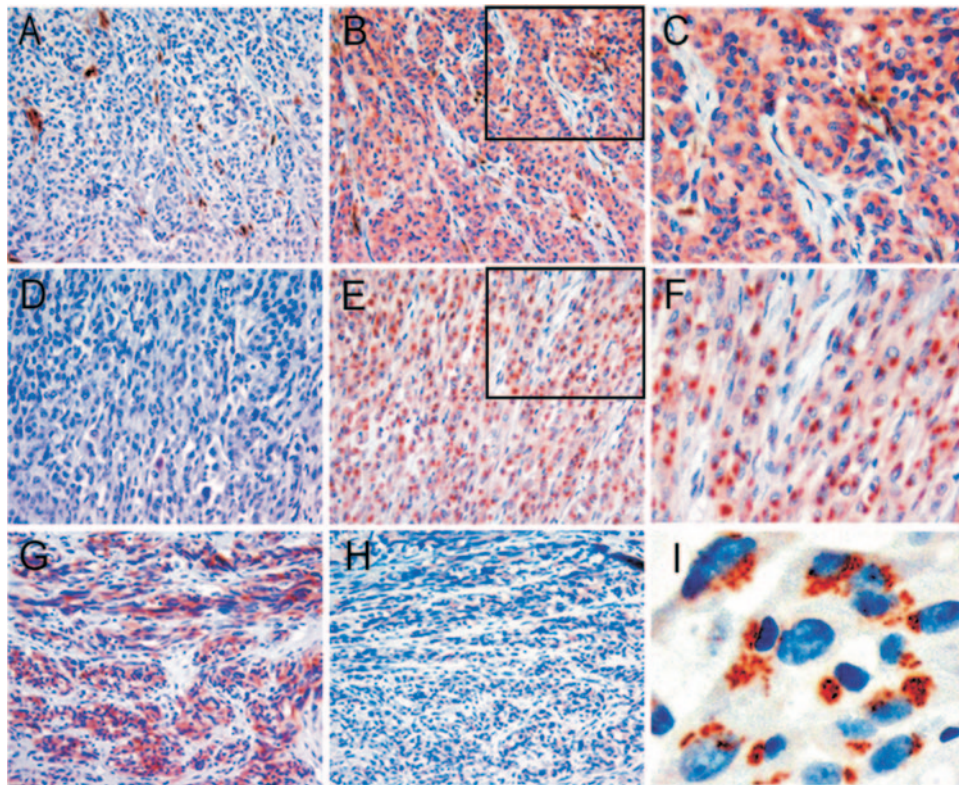


**Fig. 4.** Representative IHC of melanomas taken from the tissue microarray showing staining for PTEN and OPN. A red chromogen has been used to detect OPN and PTEN, and all sections have been counterstained with hematoxylin. (A) Primary melanoma with no PTEN expression. (B) OPN staining of corresponding primary melanoma with strong cytoplasmic and moderate punctate staining. (C) Higher magnification of boxed area in (B). (D) Primary melanoma with no PTEN. (E) OPN staining of same melanoma showing weak cytoplasmic and strong punctate staining. (F) Higher magnification of boxed area in (E). (G) Metastatic melanoma with high PTEN expression. (H) The same melanoma showing almost no OPN staining. (I) High magnification of OPN punctate staining (previously shown to correspond to the golgi and secretory vesicles) in a melanoma sample. Scale bars = 100  $\mu$ m.

**Table III.** Correlations between PTEN and OPN levels in the 67 primary melanomas as assessed by different scoring methods (percentage of cells stained, intensity of staining and the composite H-score) performed using the non-parametric Spearman test

Scoring	PTEN versus OPN punctate staining	PTEN versus OPN cytoplasmic staining	PTEN versus composite (punctate $\times$ cytoplasmic)
Percent of cells stained (P)	-0.283 ( $P = 0.020$ )*	-0.121 ( $P = 0.328$ )	-0.334 ( $P = 0.006$ )*
Intensity of staining (I)	-0.175 ( $P = 0.156$ )	0.232 ( $P = 0.058$ )	0.021 ( $P = 0.866$ )
H-score (H = P $\times$ I)	-0.388 ( $P = 0.001$ )*	0.105 ( $P = 0.396$ )	-0.308 ( $P = 0.011$ )*

Both OPN cytoplasmic and punctate staining patterns are included in the correlations. Additionally, to give an overall score for OPN including both the cytoplasmic and punctate staining, a composite value was calculated by multiplying the scores for cytoplasmic and punctate staining for each of the three scoring methods.

\*Association significant at a level of  $P < 0.05$ .

## Discussion

This is the first microarray-based study to identify genes whose expression correlates with *PTEN* genotype. The transcriptional effect of ectopic *PTEN* expression has been studied previously in lung and endometrial cancer models (62,63), though very few genes identified as downstream effectors of *PTEN* in these studies were also present in our gene list. Several factors could contribute to these differences, including the small clone sets included in the microarray analyses of others and the different experimental systems used (overexpression versus loss of function). The overall cellular effect of *PTEN* mutations in the melanoma cell lines used in this study was alluded to by GO classification of the differential gene list. For example,

DAVID analysis highlighted genes involved in regulation of transcription, cell cycle and cell proliferation. The majority of these genes showed increased expression in samples with mutated *PTEN*, supporting the tumorigenic effects of *PTEN* loss. The biological relevance of the gene list presented in this study was supported by the increased expression of *BCL3*, *HEY1*, *ITGB3*, *STAT3*, *NFKB1* and *OPN* in the *PTEN* mutant cell lines. Previous reports claim that *BCL3* promotes oncogenesis (64,65), and increased expression of *HEY1*, *ITGB3*, *STAT3*, *NFKB1* and *OPN* have been shown, or suggested, to play a role in melanoma progression (41,66–69).

Although a role for *OPN* in melanoma has been previously proposed, this is the first report of a putative link between *PTEN* and *OPN* in melanoma. A previous study in osteoclasts

showed that OPN-driven cell migration and survival was opposed by PTEN via its inhibition of the PI3K pathway (70). Inhibition of PTEN using a dominant-negative construct was found to enhance the action of OPN by augmenting the PI3K-AKT pathway. The opposing action of PTEN and OPN was confirmed in a study showing hyaluronic acid treatment of glioma cells lacking PTEN-induced OPN expression (71), and OPN expression was reduced in cells containing WT PTEN. Our data provide further evidence that a similar relationship between PTEN and OPN exists in melanoma.

The detection of increased OPN secreted from cells with mutant PTEN confirmed that increased mRNA levels also manifest at the protein level. An increase in soluble OPN is likely to enhance activation of integrin receptors, such as  $\alpha_v\beta_3$  integrin, which correlates with melanoma progression and tumorigenicity (69,72). OPN binding to surface integrins activates a number of different signal transduction pathways, including the PI3K pathway and the NF- $\kappa$ B pathway, which are both known to be important in melanomagenesis (73,74). Indeed, expression of the *ITGB3* and *NFKB1* genes was also found to be increased in PTEN mutant cell lines, supporting increased OPN activity in these cells. Thus, OPN is involved in a complex interplay of signaling pathways and appears to participate in a positive feedback loop with the PI3K pathway, as it is both activated by, and activates, this pathway (75–77). Data presented here support a role for OPN downstream of PI3K. The lack of a more pronounced reduction of *OPN* in response to PI3K inhibition may reflect the complex regulation of OPN by other signaling pathways including Ras/MEK1/2, Ras/JNK and p53 (78,79).

The inverse correlation between PTEN and OPN was confirmed in melanomas using TMAs. OPN was present in both the cytoplasm (91%) and in defined peri-nuclear spots (58%), previously identified as golgi and secretory vesicles (59–61). OPN requires phosphorylation and glycosylation in the golgi before being secreted from the cell; thus we hypothesize that the increased punctate staining of OPN in lesions without PTEN reflects the increased production, processing and secretion of OPN into the extracellular matrix. Membrane trafficking of OPN from the trans-golgi network (TGN) to the plasma membrane may be influenced by phosphatidylinositol signaling, as a subclass of PI3K has been shown to be essential for the biogenesis of exocytic vesicles from the TGN (80,81). Thus, the increased activation of PI3K in cells lacking PTEN may assist the transport of OPN from the TGN for secretion from the cell, where it can fulfill its function as a ligand to the integrin receptors. To understand the relevance of the observed punctate staining of OPN in melanocytic cells, detailed studies into its processing and trafficking are required. The tissue-specificity of the OPN transcript variants, as well as the glycosylation and phosphorylation status of the mature protein also need to be addressed in melanoma, as such post-transcriptional and post-translational modifications are thought to determine the function of OPN (82,83).

In summary, we have shown an increase of OPN when PTEN is lost and have demonstrated that PI3K influences OPN levels. However, we cannot assume that the increase in OPN is the result of the loss of the PTEN lipid phosphatase function alone. It is possible that OPN is also modulated by the protein phosphatase function of PTEN. Further experiments are required to determine which enzymatic activity of PTEN is responsible for modulating levels of OPN. We hypothesize that PTEN expression influences the modification and trafficking

of OPN to the cell surface for secretion. Thus, loss of PTEN results in increased cell secretion of OPN, thereby augmenting the tumor-promoting effects of OPN such as activation of the NF- $\kappa$ B pathway.

## Supplementary material

Supplementary material is available at *Carcinogenesis* online.

## Acknowledgements

This work was supported by the National Health and Medical Research Council of Australia, grant number 199600. N.K.H. is the recipient of a principal research fellowship of the NHMRC. L.P. is the recipient of a John Earnshaw PhD Fellowship of the Queensland Cancer Fund.

*Conflict of Interest Statement:* None declared.

## References

- Ali,I.U., Schriml,L.M. and Dean,M. (1999) Mutational spectra of *PTEN/MMAC1* gene: a tumor suppressor with lipid phosphatase activity. *J. Natl. Cancer Inst.*, **91**, 1922–1932.
- Myers,M.P., Pass,I., Batty,I.H., Van der Kaay,J., Stolarov,J.P., Hemmings,B.A., Wigler,M.H., Downes,C.P. and Tonks,N.K. (1998) The lipid phosphatase activity of PTEN is critical for its tumor suppressor function. *Proc. Natl Acad. Sci. USA*, **95**, 13513–13518.
- Krasilnikov,M.A. (2000) Phosphatidylinositol-3 kinase dependent pathways: the role in control of cell growth, survival, and malignant transformation. *Biochemistry (Mosc.)*, **65**, 59–67.
- Gu,J., Tamura,M., Pankov,R., Danen,E.H., Takino,T., Matsumoto,K. and Yamada,K.M. (1999) Shc and FAK differentially regulate cell motility and directionality modulated by PTEN. *J. Cell. Biol.*, **146**, 389–403.
- Radu,A., Neubauer,V., Akagi,T., Hanafusa,H. and Georgescu,M.M. (2003) PTEN induces cell cycle arrest by decreasing the level and nuclear localization of cyclin D1. *Mol. Cell. Biol.*, **23**, 6139–6149.
- Tamura,M., Gu,J., Takino,T. and Yamada,K.M. (1999) Tumor suppressor PTEN inhibition of cell invasion, migration, and growth: differential involvement of focal adhesion kinase and p130Cas. *Cancer Res.*, **59**, 442–449.
- Tamura,M., Gu,J., Matsumoto,K., Aota,S., Parsons,R. and Yamada,K.M. (1998) Inhibition of cell migration, spreading, and focal adhesions by tumor suppressor PTEN. *Science*, **280**, 1614–1617.
- Waite,K.A. and Eng,C. (2002) Protean PTEN: form and function. *Am. J. Hum. Genet.*, **70**, 829–844.
- Meier,F., Schitteck,B., Busch,S., Garbe,C., Smalley,K., Satyamoorthy,K., Li,G. and Herlyn,M. (2005) The RAS/RAF/MEK/ERK and PI3K/AKT signaling pathways present molecular targets for the effective treatment of advanced melanoma. *Front Biosci.*, **10**, 2986–3001.
- Krasilnikov,M., Ivanov,V.N., Dong,J. et al. (2003) ERK and PI3K negatively regulate STAT-transcriptional activities in human melanoma cells: implications towards sensitization to apoptosis. *Oncogene*, **22**, 4092–4101.
- Neudauer,C.L. and McCarthy,J.B. (2003) Insulin-like growth factor I-stimulated melanoma cell migration requires phosphoinositide 3-kinase but not extracellular-regulated kinase activation. *Exp. Cell Res.*, **286**, 128–137.
- Hess,A.R., SefTOR,E.A., SefTOR,R.E. and Hendrix,M.J. (2003) Phosphoinositide 3-kinase regulates membrane Type 1-matrix metalloproteinase (MMP) and MMP-2 activity during melanoma cell vasculogenic mimicry. *Cancer Res.*, **63**, 4757–4762.
- Hirama,M., Takahashi,F., Takahashi,K., Akutagawa,S., Shimizu,K., Soma,S., Shimanuki,Y., Nishio,K. and Fukuchi,Y. (2003) Osteopontin overproduced by tumor cells acts as a potent angiogenic factor contributing to tumor growth. *Cancer Lett.*, **198**, 107–117.
- Scatena,M., Almeida,M., Chaisson,M.L., Fausto,N., Nicosia,R.F. and Giachelli,C.M. (1998) NF-kappaB mediates alphavbeta3 integrin-induced endothelial cell survival. *J. Cell. Biol.*, **141**, 1083–1093.
- Denhardt,D.T. and Noda,M. (1998) Osteopontin expression and function: role in bone remodeling. *J. Cell. Biochem. Suppl.*, **30-31**, 92–102.
- O'Regan,A. and Berman,J.S. (2000) Osteopontin: a key cytokine in cell-mediated and granulomatous inflammation. *Int. J. Exp. Pathol.*, **81**, 373–390.

17. Faccio, R., Grano, M., Colucci, S., Zallone, A.Z., Quaranta, V. and Pelletier, A.J. (1998) Activation of alphav beta3 integrin on human osteoclast-like cells stimulates adhesion and migration in response to osteopontin. *Biochem. Biophys. Res. Commun.*, **249**, 522–525.
18. Agrawal, D., Chen, T., Irby, R., Quackenbush, J., Chambers, A.F., Szabo, M., Cantor, A., Coppola, D. and Yeatman, T.J. (2002) Osteopontin identified as lead marker of colon cancer progression, using pooled sample expression profiling. *J. Natl Cancer Inst.*, **94**, 513–521.
19. Brown, L.F., Papadopoulos-Sergiou, A., Berse, B., Manseau, E.J., Tognazzi, K., Perruzzi, C.A., Dvorak, H.F. and Senger, D.R. (1994) Osteopontin expression and distribution in human carcinomas. *Am. J. Pathol.*, **145**, 610–623.
20. Carlinfante, G., Vassiliou, D., Svensson, O., Wendel, M., Heinegard, D. and Andersson, G. (2003) Differential expression of osteopontin and bone sialoprotein in bone metastasis of breast and prostate carcinoma. *Clin. Exp. Metastasis*, **20**, 437–444.
21. Chambers, A.F., Wilson, S.M., Kerkvliet, N., O'Malley, F.P., Harris, J.F. and Casson, A.G. (1996) Osteopontin expression in lung cancer. *Lung Cancer*, **15**, 311–323.
22. Coppola, D., Szabo, M., Boulware, D., Muraca, P., Alsarraj, M., Chambers, A.F. and Yeatman, T.J. (2004) Correlation of osteopontin protein expression and pathological stage across a wide variety of tumor histologies. *Clin. Cancer Res.*, **10**, 184–190.
23. Hu, Z., Lin, D., Yuan, J. *et al.* (2005) Overexpression of osteopontin is associated with more aggressive phenotypes in human non-small cell lung cancer. *Clin. Cancer Res.*, **11**, 4646–4652.
24. Le, Q.T., Sutphin, P.D., Raychaudhuri, S., Yu, S.C., Terris, D.J., Lin, H.S., Lum, B., Pinto, H.A., Koong, A.C. and Giaccia, A.J. (2003) Identification of osteopontin as a prognostic plasma marker for head and neck squamous cell carcinomas. *Clin. Cancer Res.*, **9**, 59–67.
25. Singhal, H., Bautista, D.S., Tonkin, K.S., O'Malley, F.P., Tuck, A.B., Chambers, A.F. and Harris, J.F. (1997) Elevated plasma osteopontin in metastatic breast cancer associated with increased tumor burden and decreased survival. *Clin. Cancer Res.*, **3**, 605–611.
26. Guarino, V., Faviana, P., Salvatore, G. *et al.* (2005) Osteopontin is overexpressed in human papillary thyroid carcinomas and enhances thyroid carcinoma cell invasiveness. *J. Clin. Endocrinol. Metab.*, **90**, 5270–5278.
27. Angelucci, A., Festuccia, C., Gravina, G.L., Muzi, P., Bonghi, L., Vicentini, C. and Bologna, M. (2004) Osteopontin enhances the cell proliferation induced by the epidermal growth factor in human prostate cancer cells. *Prostate*, **59**, 157–166.
28. Oates, A.J., Barraclough, R. and Rudland, P.S. (1996) The identification of osteopontin as a metastasis-related gene product in a rodent mammary tumour model. *Oncogene*, **13**, 97–104.
29. Irby, R.B., McCarthy, S.M. and Yeatman, T.J. (2004) Osteopontin regulates multiple functions contributing to human colon cancer development and progression. *Clin. Exp. Metastasis*, **21**, 515–523.
30. Takahashi, F., Akutagawa, S., Fukumoto, H., Tsukiyama, S., Ohe, Y., Takahashi, K., Fukuchi, Y., Saijo, N. and Nishio, K. (2002) Osteopontin induces angiogenesis of murine neuroblastoma cells in mice. *Int. J. Cancer*, **98**, 707–712.
31. Kolb, A., Kleeff, J., Guweidhi, A., Esposito, I., Giese, N.A., Adwan, H., Giese, T., Buchler, M.W., Berger, M.R. and Friess, H. (2005) Osteopontin influences the invasiveness of pancreatic cancer cells and is increased in neoplastic and inflammatory conditions. *Cancer Biol. Ther.*, **4**, 740–746.
32. Adwan, H., Bauerle, T., Najajreh, Y., Elazer, V., Golomb, G. and Berger, M.R. (2004) Decreased levels of osteopontin and bone sialoprotein II are correlated with reduced proliferation, colony formation, and migration of GFP-MDA-MB-231 cells. *Int. J. Oncol.*, **24**, 1235–1244.
33. Behrend, E.I., Craig, A.M., Wilson, S.M., Denhardt, D.T. and Chambers, A.F. (1994) Reduced malignancy of ras-transformed NIH 3T3 cells expressing antisense osteopontin RNA. *Cancer Res.*, **54**, 832–837.
34. Muramatsu, T., Shima, K., Ohta, K., Kizaki, H., Ro, Y., Kohno, Y., Abiko, Y. and Shimono, M. (2005) Inhibition of osteopontin expression and function in oral cancer cell lines by antisense oligonucleotides. *Cancer Lett.*, **217**, 87–95.
35. Nemoto, H., Rittling, S.R., Yoshitake, H., Furuya, K., Amagasa, T., Tsuji, K., Nifuji, A., Denhardt, D.T. and Noda, M. (2001) Osteopontin deficiency reduces experimental tumor cell metastasis to bone and soft tissues. *J. Bone Miner Res.*, **16**, 652–659.
36. Chellaiah, M., Fitzgerald, C., Filardo, E.J., Cheresch, D.A. and Hruska, K.A. (1996) Osteopontin activation of c-src in human melanoma cells requires the cytoplasmic domain of the integrin alpha V-subunit. *Endocrinology*, **137**, 2432–2440.
37. Geissinger, E., Weisser, C., Fischer, P., Scharl, M. and Wellbrock, C. (2002) Autocrine stimulation by osteopontin contributes to antiapoptotic signalling of melanocytes in dermal collagen. *Cancer Res.*, **62**, 4820–4828.
38. Philip, S., Bulbule, A. and Kundu, G.C. (2001) Osteopontin stimulates tumor growth and activation of promatrix metalloproteinase-2 through nuclear factor-kappa B-mediated induction of membrane type 1 matrix metalloproteinase in murine melanoma cells. *J. Biol. Chem.*, **276**, 44926–44935.
39. Haqq, C., Nosrati, M., Sudilovsky, D. *et al.* (2005) The gene expression signatures of melanoma progression. *Proc. Natl Acad. Sci. USA*, **102**, 6092–6097.
40. Talantov, D., Mazumder, A., Yu, J.X., Briggs, T., Jiang, Y., Backus, J., Atkins, D. and Wang, Y. (2005) Novel genes associated with malignant melanoma but not benign melanocytic lesions. *Clin. Cancer Res.*, **11**, 7234–7242.
41. Zhou, Y., Dai, D.L., Martinka, M. *et al.* (2005) Osteopontin expression correlates with melanoma invasion. *J. Invest. Dermatol.*, **124**, 1044–1052.
42. Pavey, S., Johansson, P., Packer, L. *et al.* (2004) Microarray expression profiling in melanoma reveals a BRAF mutation signature. *Oncogene*, **23**, 4060–4067.
43. Bonneau, D. and Longy, M. (2000) Mutations of the human PTEN gene. *Hum. Mutat.*, **16**, 109–122.
44. Dennis, G. Jr, Sherman, B.T., Hosack, D.A., Yang, J., Gao, W., Lane, H.C. and Lempicki, R.A. (2003) DAVID: database for annotation, visualization, and integrated discovery. *Genome Biol.*, **4**, P3.
45. Hosack, D.A., Dennis, G. Jr, Sherman, B.T., Lane, H.C. and Lempicki, R.A. (2003) Identifying biological themes within lists of genes with EASE. *Genome Biol.*, **4**, R70.
46. Pfaffl, M.W. (2001) A new mathematical model for relative quantification in real-time RT-PCR. *Nucleic Acids Res.*, **29**, e45.
47. Gimm, O., Perren, A., Weng, L.P. *et al.* (2000) Differential nuclear and cytoplasmic expression of PTEN in normal thyroid tissue, and benign and malignant epithelial thyroid tumors. *Am. J. Pathol.*, **156**, 1693–1700.
48. Pallares, J., Bussaglia, E., Martinez-Guitarte, J.L., Dolcet, X., Llobet, D., Rue, M., Sanchez-Verde, L., Palacios, J., Prat, J. and Matias-Guiu, X. (2005) Immunohistochemical analysis of PTEN in endometrial carcinoma: a tissue microarray study with a comparison of four commercial antibodies in correlation with molecular abnormalities. *Mod. Pathol.*, **18**, 719–727.
49. Perren, A., Weng, L.P., Boag, A.H. *et al.* (1999) Immunohistochemical evidence of loss of PTEN expression in primary ductal adenocarcinomas of the breast. *Am. J. Pathol.*, **155**, 1253–1260.
50. McCarty, K.S. Jr, Miller, L.S., Cox, E.B., Konrath, J. and McCarty, K.S. Sr (1985) Estrogen receptor analyses. Correlation of biochemical and immunohistochemical methods using monoclonal antireceptor antibodies. *Arch. Pathol. Lab. Med.*, **109**, 716–721.
51. Pollock, P.M., Walker, G.J., Glendening, J.M., Que Noy, T., Bloch, N.C., Fountain, J.W. and Hayward, N.K. (2002) PTEN inactivation is rare in melanoma tumours but occurs frequently in melanoma cell lines. *Melanoma Res.*, **12**, 565–575.
52. Curtin, J.A., Fridlyand, J., Kageshita, T. *et al.* (2005) Distinct sets of genetic alterations in melanoma. *N. Engl. J. Med.*, **353**, 2135–2147.
53. Singh, K., DeVouge, M.W. and Mukherjee, B.B. (1990) Physiological properties and differential glycosylation of phosphorylated and nonphosphorylated forms of osteopontin secreted by normal rat kidney cells. *J. Biol. Chem.*, **265**, 18696–18701.
54. Takemoto, M., Yokote, K., Yamazaki, M., Ridall, A.L., Butler, W.T., Matsumoto, T., Tamura, K., Saito, Y. and Mori, S. (1999) Enhanced expression of osteopontin by high glucose in cultured rat aortic smooth muscle cells. *Biochem. Biophys. Res. Commun.*, **258**, 722–726.
55. Tsao, H., Mihm, M.C. Jr and Sheehan, C. (2003) PTEN expression in normal skin, acquired melanocytic nevi, and cutaneous melanoma. *J. Am. Acad. Dermatol.*, **49**, 865–872.
56. Slipicevic, A., Holm, R., Nguyen, M.T., Bohler, P.J., Davidson, B. and Florenes, V.A. (2005) Expression of activated Akt and PTEN in malignant melanomas: relationship with clinical outcome. *Am. J. Clin. Pathol.*, **124**, 528–536.
57. Mikhail, M., Velazquez, E., Shapiro, R. *et al.* (2005) PTEN expression in melanoma: relationship with patient survival, Bcl-2 expression, and proliferation. *Clin. Cancer Res.*, **11**, 5153–5157.
58. Whiteman, D.C., Zhou, X.P., Cummings, M.C., Pavey, S., Hayward, N.K. and Eng, C. (2002) Nuclear PTEN expression and clinicopathologic features in a population-based series of primary cutaneous melanoma. *Int. J. Cancer*, **99**, 63–67.
59. Qu, H., Brown, L.F., Dvorak, H.F. and Dvorak, A.M. (1997) Ultrastructural immunogold localization of osteopontin in human gastric mucosa. *J. Histochem. Cytochem.*, **45**, 21–33.
60. Kawashima, R., Mochida, S., Matsui, A. *et al.* (1999) Expression of osteopontin in Kupffer cells and hepatic macrophages and Stellate cells in rat liver after carbon tetrachloride intoxication: a possible factor for

- macrophage migration into hepatic necrotic areas. *Biochem. Biophys. Res. Commun.*, **256**, 527–531.
61. Verhulst, A., Persy, V.P., Van Rompay, A.R., Verstrepen, W.A., Helbert, M.F. and De Broe, M.E. (2002) Osteopontin synthesis and localization along the human nephron. *J. Am. Soc. Nephrol.*, **13**, 1210–1218.
  62. Matsushima-Nishiu, M., Unoki, M., Ono, K., Tsunoda, T., Minaguchi, T., Kuramoto, H., Nishida, M., Satoh, T., Tanaka, T. and Nakamura, Y. (2001) Growth and gene expression profile analyses of endometrial cancer cells expressing exogenous PTEN. *Cancer Res.*, **61**, 3741–3749.
  63. Hong, T.M., Yang, P.C., Peck, K., Chen, J.J., Yang, S.C., Chen, Y.C. and Wu, C.W. (2000) Profiling the downstream genes of tumor suppressor PTEN in lung cancer cells by complementary DNA microarray. *Am. J. Respir. Cell. Mol. Biol.*, **23**, 355–363.
  64. Zhao, S., Martin, A.M., Meek, D.W. and Perkins, N.D. (2003) p53 represses cyclin D1 transcription through downregulation of Bcl-3 and inducing increased association of the p52 NF-kappaB subunit with histone deacetylase 1. *Mol. Cell. Biol.*, **23**, 4713–4727.
  65. Zhao, Y., Ramakrishnan, A., Kim, K.E. and Rabson, A.B. (2005) Regulation of Bcl-3 through interaction with the Lck tyrosine kinase. *Biochem. Biophys. Res. Commun.*, **335**, 865–873.
  66. Hoek, K., Rimm, D.L., Williams, K.R. *et al.* (2004) Expression profiling reveals novel pathways in the transformation of melanocytes to melanomas. *Cancer Res.*, **64**, 5270–5282.
  67. McNulty, S.E., del Rosario, R., Cen, D., Meyskens, F.L. Jr and Yang, S. (2004) Comparative expression of NFkappaB proteins in melanocytes of normal skin vs. benign intradermal naevus and human metastatic melanoma biopsies. *Pigment Cell Res.*, **17**, 173–180.
  68. Niu, G., Bowman, T., Huang, M., Shivers, S., Reintgen, D., Daud, A., Chang, A., Kraker, A., Jove, R. and Yu, H. (2002) Roles of activated Src and Stat3 signaling in melanoma tumor cell growth. *Oncogene*, **21**, 7001–7010.
  69. Seftor, R.E. (1998) Role of the beta3 integrin subunit in human primary melanoma progression: multifunctional activities associated with alpha(v)beta3 integrin expression. *Am. J. Pathol.*, **153**, 1347–1351.
  70. Sugatani, T., Alvarez, U. and Hruska, K.A. (2003) PTEN regulates RANKL- and osteopontin-stimulated signal transduction during osteoclast differentiation and cell motility. *J. Biol. Chem.*, **278**, 5001–5008.
  71. Kim, M.S., Park, M.J., Moon, E.J., Kim, S.J., Lee, C.H., Yoo, H., Shin, S.H., Song, E.S. and Lee, S.H. (2005) Hyaluronic acid induces osteopontin via the phosphatidylinositol 3-kinase/Akt pathway to enhance the motility of human glioma cells. *Cancer Res.*, **65**, 686–691.
  72. Felding-Habermann, B., Mueller, B.M., Romerdahl, C.A. and Cheresch, D.A. (1992) Involvement of *integrin alpha V* gene expression in human melanoma tumorigenicity. *J. Clin. Invest.*, **89**, 2018–2022.
  73. Das, R., Mahabeshwar, G.H. and Kundu, G.C. (2003) Osteopontin stimulates cell motility and nuclear factor kappaB-mediated secretion of urokinase type plasminogen activator through phosphatidylinositol 3-kinase/Akt signaling pathways in breast cancer cells. *J. Biol. Chem.*, **278**, 28593–28606.
  74. Rangaswami, H., Bulbule, A. and Kundu, G.C. (2005) JNK1 differentially regulates osteopontin-induced nuclear factor-inducing kinase/MEKK1-dependent activating protein-1-mediated promatrix metalloproteinase-9 activation. *J. Biol. Chem.*, **280**, 19381–19392.
  75. Zhang, G.X., Zhao, Z.Q., Wang, H.D. and Hao, B. (2004) Enhancement of osteopontin expression in HepG2 cells by epidermal growth factor via phosphatidylinositol 3-kinase signaling pathway. *World J. Gastroenterol.*, **10**, 205–208.
  76. Ariztia, E.V., Subbarao, V., Solt, D.B., Rademaker, A.W., Iyer, A.P. and Oltvai, Z.N. (2003) Osteopontin contributes to hepatocyte growth factor-induced tumor growth and metastasis formation. *Exp. Cell. Res.*, **288**, 257–267.
  77. Junaid, A. and Amara, F.M. (2004) Osteopontin: correlation with interstitial fibrosis in human diabetic kidney and PI3-kinase-mediated enhancement of expression by glucose in human proximal tubular epithelial cells. *Histopathology*, **44**, 136–146.
  78. Crawford, H.C., Matrisian, L.M. and Liaw, L. (1998) Distinct roles of osteopontin in host defense activity and tumor survival during squamous cell carcinoma progression *in vivo*. *Cancer Res.*, **58**, 5206–5215.
  79. Li, C.M., Kim, C.E., Margolin, A.A. *et al.* (2004) CTNNB1 mutations and overexpression of Wnt/beta-catenin target genes in WT1-mutant Wilms' tumors. *Am. J. Pathol.*, **165**, 1943–1953.
  80. Jones, S.M., Alb, J.G. Jr, Phillips, S.E., Bankaitis, V.A. and Howell, K.E. (1998) A phosphatidylinositol 3-kinase and phosphatidylinositol transfer protein act synergistically in formation of constitutive transport vesicles from the trans-Golgi network. *J. Biol. Chem.*, **273**, 10349–10354.
  81. Meunier, F.A., Osborne, S.L., Hammond, G.R., Cooke, F.T., Parker, P.J., Domin, J. and Schiavo, G. (2005) Phosphatidylinositol 3-kinase C2alpha is essential for ATP-dependent priming of neurosecretory granule exocytosis. *Mol. Biol. Cell.*, **16**, 4841–4851.
  82. Al-Shami, R., Sorensen, E.S., Ek-Rylander, B., Andersson, G., Carson, D.D. and Farach-Carson, M.C. (2005) Phosphorylated osteopontin promotes migration of human choriocarcinoma cells via a p70 S6 kinase-dependent pathway. *J. Cell. Biochem.*, **94**, 1218–1233.
  83. Young, M.F., Kerr, J.M., Termine, J.D., Wewer, U.M., Wang, M.G., McBride, O.W. and Fisher, L.W. (1990) cDNA cloning, mRNA distribution and heterogeneity, chromosomal location, and RFLP analysis of human osteopontin (OPN). *Genomics*, **7**, 491–502.

Received January 27, 2006; revised March 13, 2006;  
accepted March 15, 2006